Potential Use of Cellulose from Kenaf in Polymer Electrolytes Based on MG49 Rubber Composites

Serawati Jafirin, Ishak Ahmad,* and Azizan Ahmad

The possibility of using cellulose from kenaf as reinforcing fibres in lithium-conducting composite polymer electrolytes based on 49% poly(methyl methacrylate)-grafted natural rubber and $LiCF_3SO_3$ has been explored. Cellulose was extracted from kenaf bast fibres by a two-step chemical treatment, specifically an alkali treatment and a bleaching process. High-performance composite polymer electrolytes were prepared by solution casting with various compositions of cellulose (0-10 wt%). Scanning electron microscopy was used for morphological studies of the kenaf fibres at each stage of treatment. The morphology of the electrolytes showed a good dispersion of the cellulose fibres. Infrared spectroscopy showed significant interactions between Li^+ ions from the salt and the C=O and C-O-C groups of methyl methacrylate. X-ray diffraction analysis showed that the crystallinity of the polymer host increased upon addition of cellulose and decreased upon addition of salt. Composite electrolytes with 4 wt% cellulose exhibited the best mechanical performance with 10.9 MPa and 995 MPa for tensile strength and Young's modulus, respectively. The electrolyte films were analyzed by electrochemical impedance spectroscopy and the optimum value of ionic conductivity of SPE with cellulose was 5.3×10^{-7} Scm^{-1}. The addition of cellulose involved a weak decrease of the conductivity, which might be due to interactions between cellulose, polymer, and $LiCF_3SO_3$. The incorporation of cellulose fibres in polymer electrolytes provides a high reinforcing effect at an acceptable level of ionic conductivity.

Keywords: Composite polymer electrolytes; Kenaf; Cellulose; Ionic conductivity; Mechanical properties

*Contact information: Polymer Research Centre (PORCE), School of Chemical Science and Food Technology, Universiti Kebangsaan Malaysia, 43600, Bangi, Selangor Darul Ehsan, Malaysia; *Corresponding author: gading@ukm.my*

INTRODUCTION

Cellulose is the most abundant renewable resource available today and the most promising feedstock for industry in the future. Cellulose, an organic component of the primary cell wall of green plants with formula $(C_6H_{10}O_5)_n$, is the most common organic compound on earth (Li *et al*. 2009). The characteristics of cellulose fibres has contributed to a broad range of potential applications, including use as raw materials for paper-making, food, and additives in the optical and pharmaceutical industries (Li *et al*. 2009). Cellulose has been investigated and exploited for many decades because of its attractive chemical and physical properties. Currently, the application of cellulose and its derivatives has been further expanded to include production in the form of biomass filler for the preparation of composite polymer electrolytes (Regiani *et al*. 2001; Nair *et al*. 2009; Alloin *et al*. 2010; Samsudin and Isa 2012).

These fibres can be used as reinforcing agents in polymer electrolytes to deliver better mechanical strength for application as separators in lithium-based batteries. The

synthetic fillers that are added in polymer electrolytes are non-biodegradable. This practice leads to problems in the disposal of the electrolytes. In contrast, replacing the synthetic fillers with natural fibres will overcome this problem. Thus, the introduction of cellulose in polymer electrolytes as an alternative to traditional glass fibres such as Al_2O_3 and TiO_2 (Alloin *et al*. 2010) in commercial composite materials has drawn much attention.

Kenaf (*Hibiscus cannabinus*) is a plant that belongs to the Malvaceae family and is grown commercially in many places, including Malaysia. Kenaf consists of two separate parts, which are bast and core. Usually, fibres are derived from the bast because it has attractive mechanical properties. Kenaf fibres derived from the outer fibrous bark, the bast, contains about 30% to 63% cellulose (Rowell and Stout 1998; Bismark *et al*. 2005; Kargarzadeh *et al*. 2012). The high percentage of cellulose makes kenaf suitable for cellulose extraction. Furthermore, the use of kenaf or lignocellulose fibres as organic filler is a wise step in replacing inorganic fillers because it is a cheap, easily available, and almost unlimited resource, enabling the improvement of the mechanical properties of composites without being harmful to human health (Swingle *et al*. 1978).

Various chemical treatments have been applied to improve the mechanical performance of these natural fibres in terms of their wettability and to modify their microstructure, surface morphology, and tensile strength before they can be used in solid polymer electrolytes (Rout *et al*. 2001). The cellulose chains are biochemically synthesized in the form of microfibrils that contain amorphous and crystalline phases (Li *et al*. 2009). The crystalline regions are important to produce good mechanical properties, while the amorphous regions are crucial to enhance ion mobility in polymer electrolytes (Pandey *et al*. 2009). By contrast, the crystalline phase will restrict the motion of the Li^+ ion, and hence decrease its conductivity.

Solid polymer electrolytes (SPEs) have been used as ion carriers in lithium-based secondary batteries. SPEs have the potential to be used as rechargeable batteries, fuel cells, and light-emitting fuels, and in many other applications in electrochemistry (Rowell and Stout 1998). However, the use of solid polymer electrolytes is very limited due to low ionic conductivity at ambient temperature, some leakage problems and pressure-induced deformations (Nik Aziz *et al*. 2010) compared to other polymer electrolytes. One of the main objectives in polymer research is to develop polymer systems with high ionic conductivity combined with encouraging mechanical properties.

Recently, modified natural rubber (NR)-based SPEs have grabbed the attention of many researchers due to attractive attributes such as a low glass transition temperature T_g, soft elastomer characteristics at room temperature, and good elasticity (Ahmad *et al*. 2011; Latif *et al*. 2006; Low *et al*. 2010). A suitable elasticity can result in thin and flexible films. Furthermore, modified NR gives an excellent contact between an electrolytic layer and an electrode in battery systems and can act as a polymeric solvent. Modified NR, similar to poly(methyl methacrylate)-grafted natural rubber (MG), contains oxygen atoms that can act as electron donor atoms in the structure of the polymer host. Oxygen atoms with a lone pair of electrons form a coordinate bond with Li^+ ions from a salt and a polymer complex. MG films are free-standing to a large extent, elastic, and flexible. Figure 1 shows the structure of an MG monomer (Su'ait *et al*. 2009b).

In the present work, 49% MG (MG49) was doped with lithium triflate salt. Cellulose fibres from kenaf were used as a reinforcing agent for the preparation of a composite polymer electrolyte (Schroers *et al*. 2004).

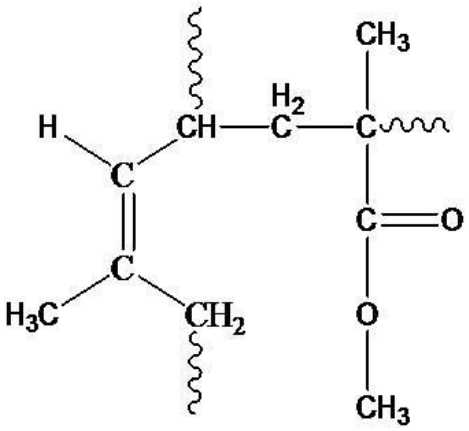

Fig. 1. Structure of an MG monomer

In case of cellulose as filler's surface, the OH group of cellulose is expected to favor interactions (via hydrogen bonding) with $CF_3SO_3^-$ ion or with the MG49 group (Fig. 2). The interaction between cellulose fibres and MG49 results in better mechanical properties.

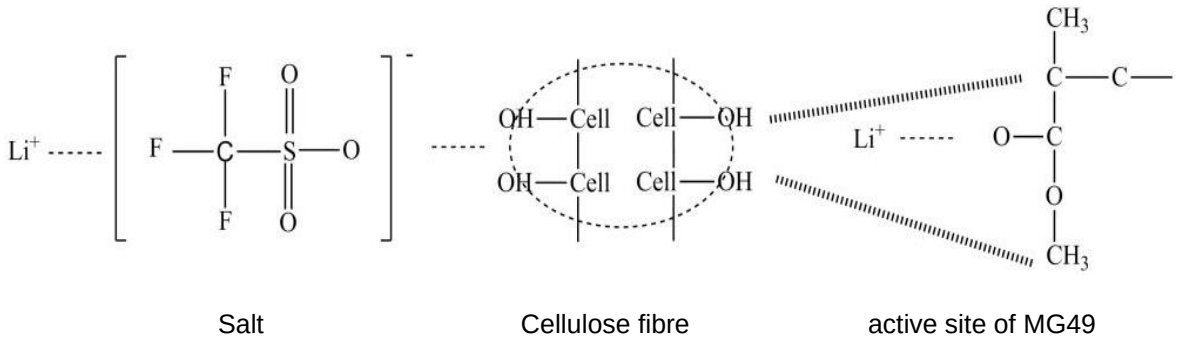

Fig. 2. Interaction of active site of MG49 and cellulose fibre or salt

Many researchers have employed natural fibres for the preparation of polymer electrolytes, used either as filler or as a polymer host. Recently, SPEs made from natural renewable biomass, such as sisal, cotton, ramie (Alloin *et al*. 2010), cellulose (Chiappone *et al.* 2011; Nair *et al.* 2009), tunicate, a sea animal (Azizi Samir *et al*. 2004a, 2004b; Schroers *et al*. 2004; Azizi Samir *et al*. 2005), carboxymethyl cellulose (Nik Aziz *et al*. 2010; Rozali *et al*. 2012; Samsudin and Isa 2012), cellulose derivatives (Regiani *et al.* 2001), and chitosan (Pawlicka *et al.* 2008; Mobarak *et al*. 2013) have been extensively investigated because of their low environmental impact and low cost compared with synthetic polymer electrolytes, which involve the depletion of fossil resources.

Although a number of research studies using natural fibres in SPEs have been performed, no investigations regarding the use of cellulose from kenaf have been reported. There is no study regarding the addition of cellulose from kenaf in polymer electrolyte yet. A previous study used cellulose from tunicate, sisal, cotton, ramie and chitosan (Azizi Samir *et al*. 2004a, 2004b; Alloin *et al*. 2010; Pawlicka *et al.* 2008). There is also no study on the addition of cellulose in grafted natural rubber because poly(ethylene oxide) is often used. Other than that, polymer composites and composite polymer electrolytes were different in terms of application. Here, the potential of using cellulose from kenaf in modified NR-based SPEs is studied extensively by means of mechanical and conductivity measurements. Moreover, investigations of the chemical

and physical properties of cellulose in SPEs are carried out to analyze their suitability as a reinforcing agent.

EXPERIMENTAL

Materials

Kenaf fibres were supplied by Kenaf Fibres Industry Sdn. Bhd. (Malaysia). Sulphuric acid (98%), sodium hydroxide (99%), sodium chlorite (80%), and glacial acetic acid (99.5%), were purchased from SYSTERM-chemAR (Malaysia) and Sigma-Aldrich (Germany). Amino-silane was supplied by Dow Corning. Tetrahydrofuran (THF) was purchased from JT Baker. MG49 rubber (~15,000 Mw) was commercially obtained from Green HPSP (M) Sdn. Bhd. Lithium triflate ($LiCF_3SO_3$) salt was supplied by Fluka. All chemicals were used without further purification.

Preparation of Cellulose from Kenaf

The extraction of cellulose consisted of two steps; the first was an alkali treatment, and the second was a bleaching process (Kargarzadeh *et al*. 2012). Prior to the chemical treatment, the kenaf fibres were cut into small pieces. Briefly, kenaf fibres were treated with 4 wt% NaOH solution in a round bottom flask under mechanical stirring at 80 °C for 3 h. For all of the treatments, the process was repeated three times and refluxing was conducted throughout the entire time of the process. The solution was then filtered several times using distilled water to remove the alkali component. After that, bleaching was performed four times with 1.7 w/v% of sodium chlorite and acetic buffer solution (2.7 g NaOH and 7.5 mL glacial acetic acid in 100 mL distilled water) in a stoppered flask under mechanical stirring. Five w/v% fibres were added and subjected to a reflux process at 80 °C under mechanical stirring for 4 h. The fibres and the solution were allowed to cool and then were filtered using excess distilled water, followed by drying in air (Siqueira *et al*. 2010). A silane treatment was conducted after the bleaching treatment with 5% silane.

The treatment of cellulose with silanes was performed in a 100 mL mixture of H_2O and silane. The concentration of the silane coupling agent was 0.5%. Acetic acid was added to adjust the pH to 6.0-7.0.The solution was then stirred for 15 min to ensure complete silane hydrolysis, after which the cellulose samples were added. The samples were soaked for 1 h, and then removed from the solutions and washed with distilled water. The cellulose sample was then dried at room temperature for 24 h. Silane was used to reduce the number of OH groups in cellulose. Hydroxyl group of cellulose tends to interact with Li+ from salt. The interaction will restrict the mobility of Li+ salt and decrease the ionic conductivity.

SPEs Film Processing

All polymer electrolyte samples were prepared by solution casting (Schroers *et al*. 2004; Su'ait *et al*. 2009b). Composite polymer electrolytes were prepared in THF medium. Three grams of MG49 rubber was sliced into grains and dissolved in conical flasks containing THF. After 24 h, the solution was stirred magnetically for the next 24 h until complete dissolution of MG49 was achieved, resulting in a clear viscous solution. Then, 20 wt% $LiCF_3SO_3$ salt was stirred in the THF solution for 12 h, until a homogenous solution was obtained. Subsequently, the salt solution was added to the

MG49 solutions under continuous stirring for the next 24 h. THF and cellulose were added into a conical flask, and a cellulose suspension formed after multiple solvent exchanges (water, acetone, THF) and centrifugation. The THF suspension of cellulose was added to the MG49/salt solution in a conical flask under continuous stirring for 24 h to obtain a homogeneous solution. The solution was casted onto a petri dish and allowed to evaporate in a fume hood at room temperature for 24 h. Then, these films were further dried under vacuum oven for the next 24 h to remove any trace amount of the residual solvent. The samples were then stored in desiccators for further use.

Characterization

Scanning electron microscopy (SEM)

The morphology of the fibres after each treatment was investigated using a Zeiss Supra 55VP scanning electron microscope with a magnification of 100×. All samples were sputter-coated with gold before observation to prevent charging. A coating time of 1 min and 20 mA current were used. The morphology of the polymer electrolytes was investigated using the same instrument with a magnification of 500×.

ATR-FTIR characterization

Attenuated total reflectance Fourier transform infrared (ATR-FTIR) spectra were recorded by a computer-interfaced Perkin-Elmer Spectrum 2000 spectrometer that was used to examine the changes in the functional groups induced by the various treatments. The samples were ground and analyzed in transmittance mode within the wavenumber range of 4000 to 600 cm^{-1} at a resolution of 4 cm^{-1}.

X-ray Diffraction (XRD) Analysis

An XRD diffractometer model D-5000 Siemens was used to observe the appearance and disappearance of the crystalline and amorphous phases as a function of salt content. The data were collected within a range of the diffraction angle 2θ from 2° to 50° in steps of 0.04°. The wavelength of the incident Cu Kα radiation was 0.1541 nm, and the operation voltage and current were 40 kV and 40 mA, respectively. The fibres were characterized, and the crystallinity index (CrI) was determined using the following equation (Labuschagne *et al.* 2008),

$$CI(\%) = \frac{(I_{peak} - I_{am})}{I_{peak}} \times 100 \quad (1)$$

where I_{peak} and I_{am} are the intensities of the highest peak and the amorphous diffraction.

Mechanical properties

A tensile test machine (Instron 5566, USA) was used to evaluate the mechanical performance of the polymer electrolytes. This process was conducted at room temperature according to ASTM D882. A crosshead speed of 50 mm/min, an initial grip distance of 40 mm, and a load of 50 N were applied to perform this test. The samples were cut into a dumbbell shape, and an average value was determined based on five replicates for each sample. The tensile tests were analysed using Bluehill software.

Ionic conductivity

The ionic conductivity measurements were carried out by electrochemical impedance spectroscopy (EIS) using a high-frequency resonance analyzer (HFRA) model

1255 with applied frequencies from 0.1 Hz to 1 MHz at a perturbation voltage of 1000 mV. The disc-shaped sample of 16 mm in diameter was sandwiched between two stainless steel block electrodes. All experiments were conducted at room temperature (Schroers *et al*. 2004).

RESULTS AND DISCUSSION

Cellulose Morphology

Figure 3 presents SEM micrographs of kenaf fibres after different stages of treatment. The figure indicates that the morphology of the kenaf fibres changed with the chemical processing. Figure 3a shows that the raw kenaf fibres had a rough surface. The untreated kenaf fibres were bonded together by massive cement materials. The diameter of the raw kenaf fibres ranged from 60 ± 2.7 to 122 ± 3.1 µm.

However, after undergoing alkali treatment, the rough surfaces of raw fibers were devastated. During alkali treatment, most of the hemicelluloses were hydrolyzed and became water soluble. This treatment partially removed the hemicelluloses, lignin, wax, and oil covering the external surface of the fibre cell walls. The treatment also depolymerised the cellulose and exposed a short length of crystallites (Kaushik *et al*. 2010). Almost all impurities were removed from the fibre surface, which induced the separation of fibre bundles into individual fibres (Kargarzadeh *et al*. 2012). The diameter of the fibres also decreased to a range of 12 ± 2.2 to 80 ± 3.8 µm.

Figure 3c shows the morphology of the bleached kenaf fibres and significant physical changes of the fibril surface. During bleaching, the colour of the kenaf fibres changed to white and the surface became smoother. This can be attributed to the fact that the treatment removes most of the lignin. Lignin is composed of hydroxyl phenyl propane. The molecules are connected to each other by partial carbon-carbon bonds in a helical structure. The bleaching agent enhances the hydrophilicity by forming carboxylic, carbonyl, and hydroxyl groups that can be dissolved in an alkaline medium, leaving behind pure cellulose fibres (Pandey *et al*. 2009). The penetration of bleaching agents inside cellulose bundles leads to further defibrillation to a single fibril. The diameter of the bleached fibres is then further reduced, ranging from 6 ± 4.3 to 12 ± 2.8 µm, much smaller than the untreated and alkali-treated fibres.

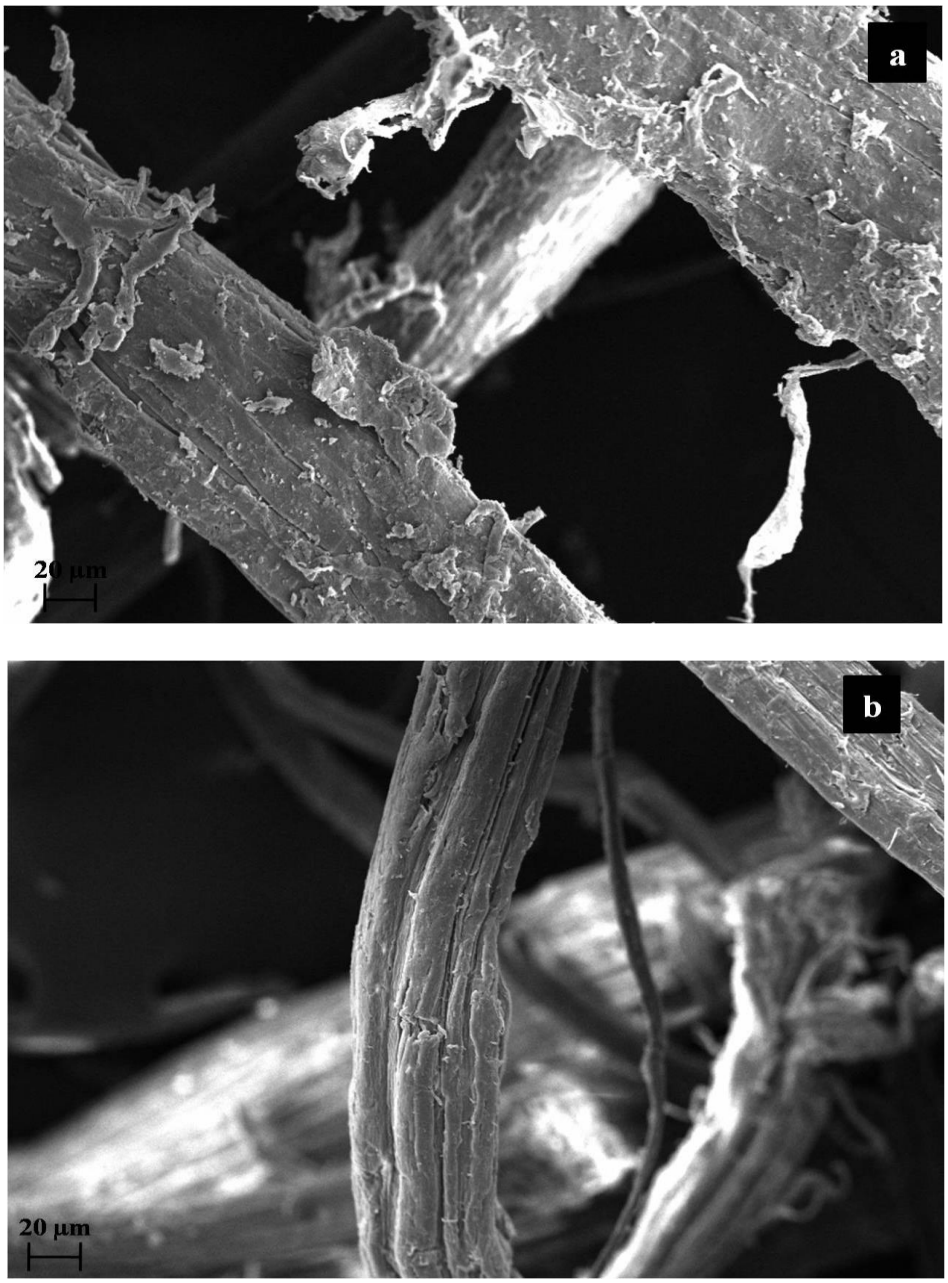

Fig. 3a & b. SEM micrograph of a) raw kenaf; b) alkali-treated kenaf

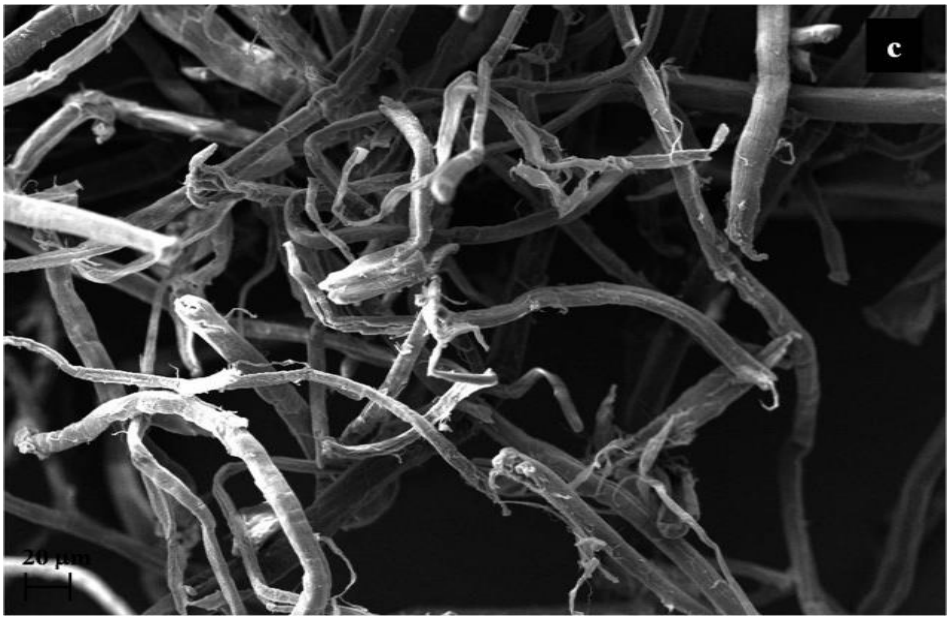

Fig 3c. SEM micrographs bleached kenaf

ATR-FTIR Characterization

ATR-FTIR spectroscopy was used to determine the vibrational energy of covalent bonds in the polymer host, which enabled the determination of the interactions existing in the polymer salt complexes, as shown in Fig. 4. The absorbance peaks at 3500 to 3400 cm^{-1} and at 1640 to 1660 cm^{-1} can be attributed to stretching and bending vibrations, respectively, of the OH group of cellulose (Kargarzadeh *et al*. 2012). The peaks observed in the range of 1640 to 1660 cm^{-1} only appeared in the FTIR spectra of SPEs with added kenaf fibres (Fig. 4c and 4d) and indicated the presence of OH groups in the cellulose. Likewise, peaks at 2900 to 2800 cm^{-1} appeared after the addition of fibres and can be attributed to CH groups in the cellulose.

The main focus of FTIR studies of polymer electrolytes has been the carbonyl (C=O) region at 1750 to 1720 cm^{-1} and the ether (C-O-C) region at 1300 to 1000 cm^{-1}, originating from MG49 (Su'ait *et al.* 2009b; Kamisan *et al*. 2011). In this work, oxygen atoms (C=O) were found to act as electron donors and formed a coordinate bond with Li ions from the salt, thereby forming polymer-salt complexes. The carbonyl group showed a very strong peak at 1750 to 1720 cm^{-1} that was shifted to lower wavenumbers by 5 to 20 cm^{-1} in the polymer-salt complexes. The intensity of the C=O peak originating from methyl methacrylate (MMA) was reduced and shifted to lower wavenumbers, from 1727 cm^{-1} to 1722 cm^{-1}, after the addition of the salt. The shifting of the peak indicated the interaction between lithium ions and oxygen atoms (C=O) in MMA. The absorption band appearing in the range of 1065 to 1147 cm^{-1} was shifted to lower wavenumbers in polymer-salt complexes after the addition of fibres. This was attributed to C-O stretching and C-H rocking vibrations of the pyranose ring skeleton (Alemdar and Sain 2008).

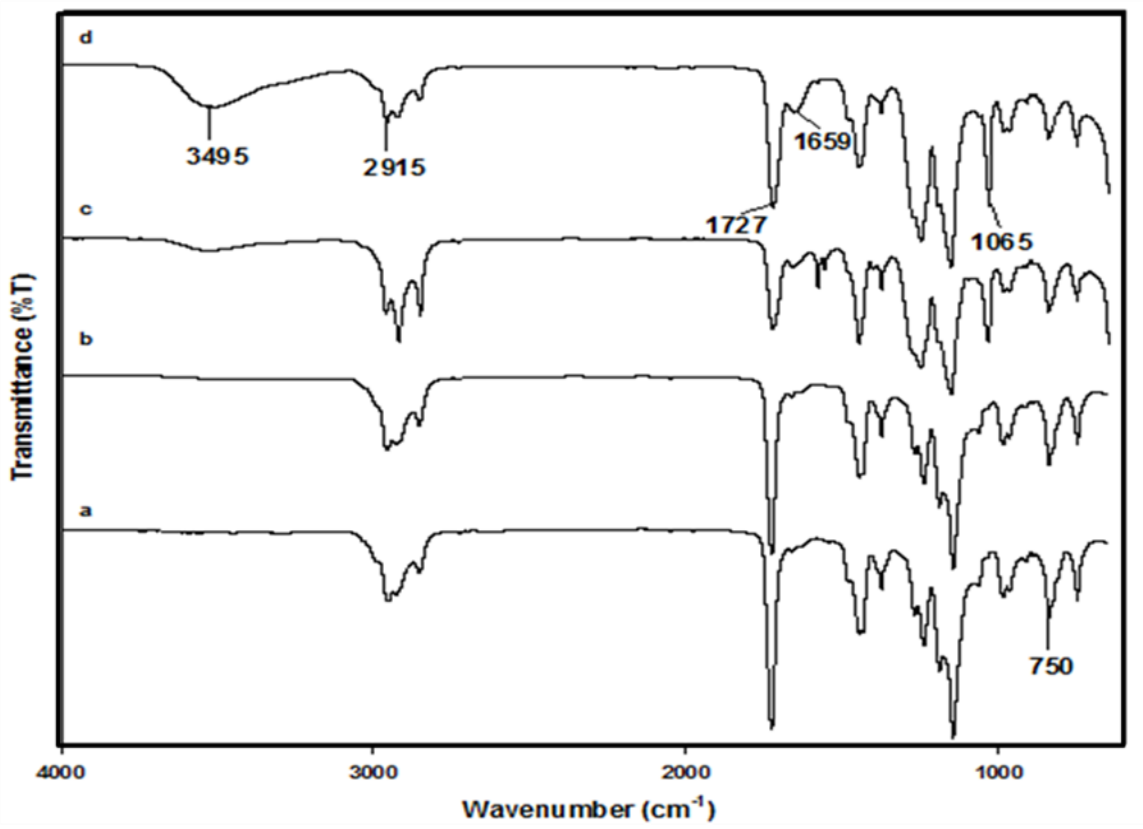

Fig. 4. FTIR spectra of SPE: a) MG49; b) MG49+salt; c) MG49+fibre+salt; and d) MG49+fibre

Mechanical Properties

The mechanical properties of SPE composites are primarily associated with the geometrical ratio of the fibres, the processing methods, the compatibility of the cellulose fibres with the matrix MG49, and the filler-to-filler interaction (Pandey *et al*. 2009). The tensile strength of SPEs with different percentages of fibre loading was measured, and the results are shown in Figs. 5a and 5b. It was found that the tensile strength (Fig. 5a) of SPE increased from 0 to 4 wt% cellulose fibre loading. SPEs reinforced by 4 wt% fibres presented the highest tensile strength among all investigated compositions of composite polymer electrolytes, 10.9 MPa. SPEs with 4 wt% cellulose fibres resulted in the optimum filler loading with the highest tensile strength and modulus due to good dispersion of cellulose in the matrix. SPEs reinforced by cellulose fibres had higher values of tensile strength compared to those without cellulose. In a previous study, the crystallinity of the fibres was found to increase after alkali and bleaching treatment (Kargarzadeh *et al.* 2012). The high crystallinity of cellulose fibres in SPEs improved and enhanced the mechanical properties of SPE films.

The Young's modulus (Fig. 5b) also tended to increase after the addition of cellulose. Again, SPEs with 4 wt% cellulose showed the optimum value of the modulus (995 MPa), much higher than in the case of unfilled SPEs (380 MPa). The crystalline regions in cellulose resulted in a reinforcement effect for the SPEs because of a rigid percolating cellulose fibre network that was assumed to have formed through the strong hydrogen bonds in cellulose fibres (Azizi Samir *et al*. 2004b). The reinforcement effect can also be explained by an increase of uniformity that contributes to the increase in strength on account of the removal of impurities after the alkali and bleaching process.

Interestingly, the Young's modulus can also be considered high for a small amount of fibres upon addition of $LiCF_3SO_3$. Thus, the significant increase of the tensile strength and Young's modulus might be related to a stabilizing effect of the salt, which might lead to a better dispersion of cellulose inside the polymer matrix (Schroers *et al*. 2004).

However, when the percentage of cellulose fibres was further increased above 4 wt%, the tensile strength and the Young's Modulus of the SPEs gradually decreased. The rigidity of this network depends on the concentration of the filler with respect to the filler/filler interaction through hydrogen bonding (Azizi Samir *et al*. 2004b). Nonetheless, due to a non-uniform distribution of cellulose in the matrix, there was a certain degree of agglomeration. Hence, the mechanical stability of SPEs decreased above 4 wt% of cellulose fibres.

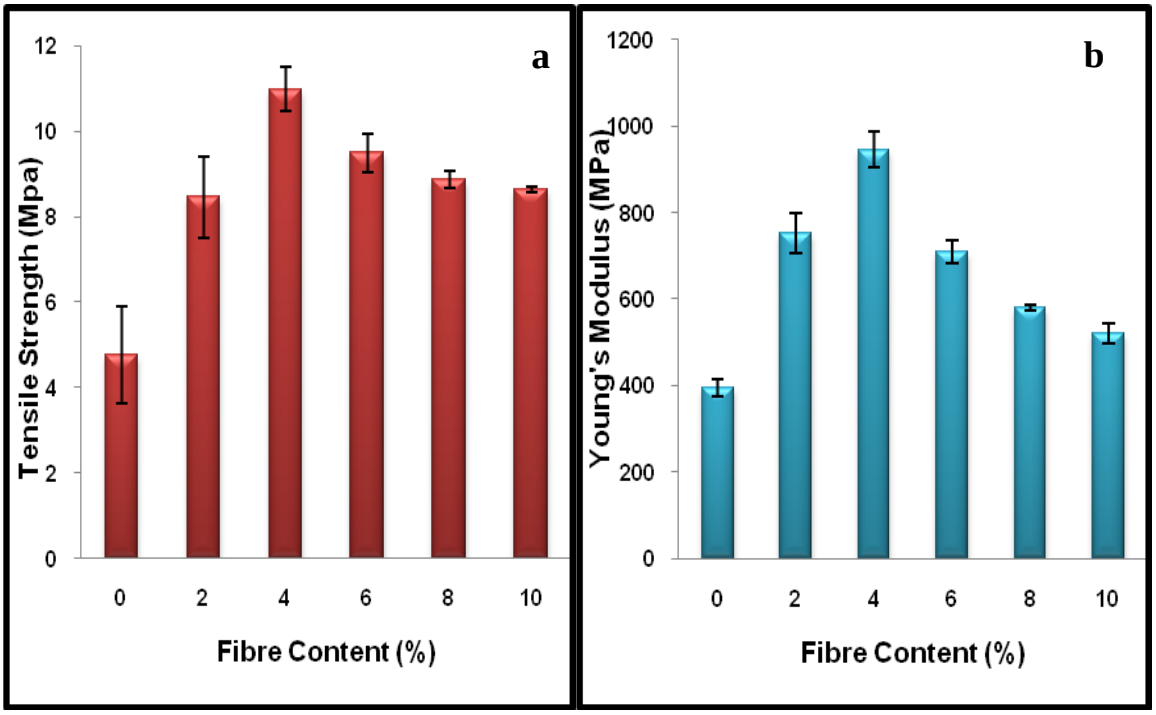

Fig. 5. Graph of the a) tensile strength and b) Young's modulus of SPEs with respect to fibre content

X-ray Diffraction (XRD) Analysis

The XRD analysis was done based on the optimum composition for tensile strength and Young's modulus which is at 4 wt%. Figure 6 shows the XRD patterns of SPE MG49-$LiCF_3SO_3$. Generally, all diffractograms showed well-defined crystalline peaks around 2θ = 29° and 30° to 50º. As shown, the magnitude of the peaks located at 29°, 30° to 50° decreased with the addition of salt. In contrast, the magnitude of these peaks increased after addition of cellulose fibre, which was attributed to an increase of crystallinity.

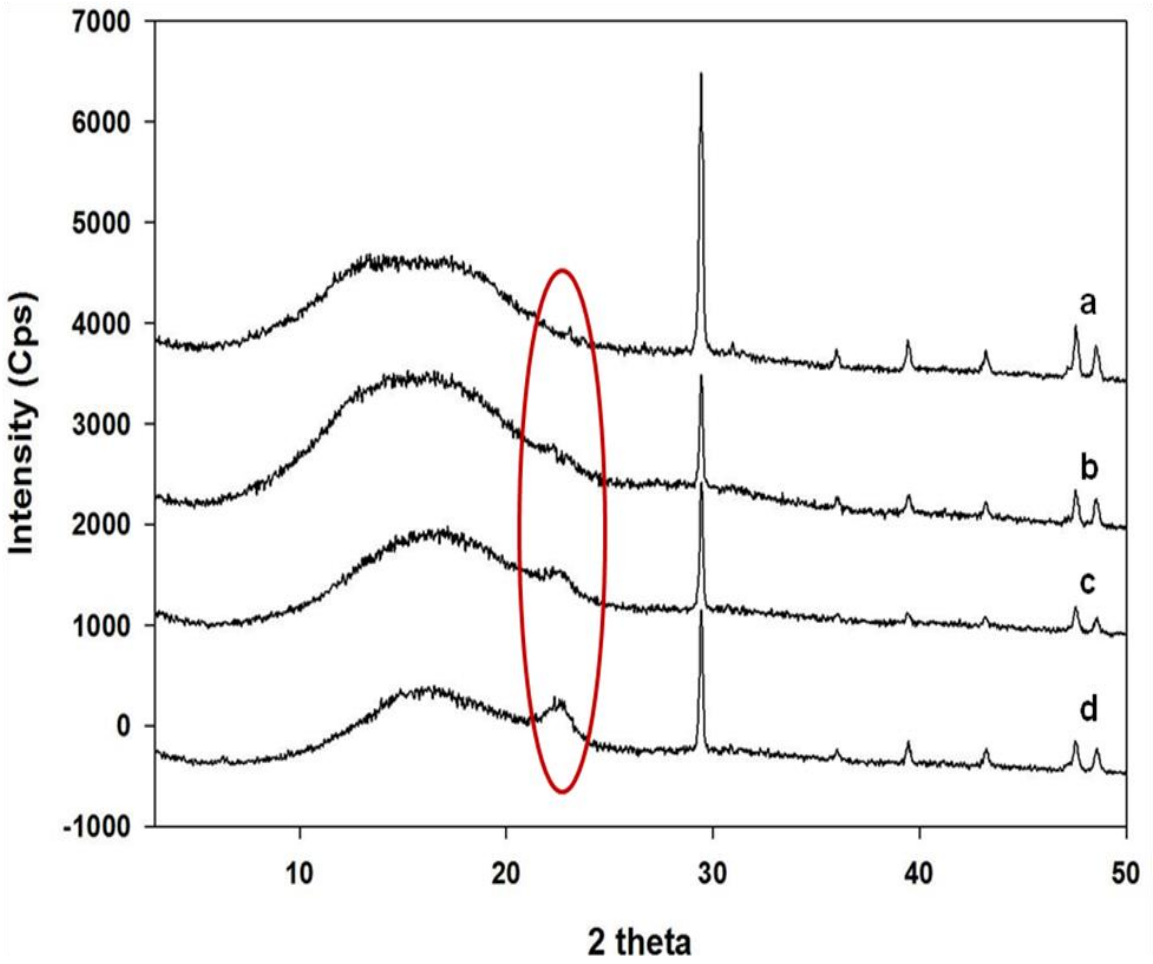

Fig. 6. X-ray diffraction patterns of SPE: a) MG49; b) MG49+salt; d) MG49+salt+4 wt% fibre; e) MG49+salt+8 wt% fibre

On the other hand, a broad hump corresponding to the amorphous region appeared in the range 12° to 22°. In a manner similar to that of the crystalline peaks, the peaks also became broader after the addition of salt. As shown in Fig. 6, the magnitude of the peaks located at 29° increased with the addition of cellulose. There was also a new peak appearing around 2θ = 22.5° after addition of cellulose. The peak around 2θ= 22.5° corresponds to (002) planes of the cellulose group, and this peak could be observed only after addition of cellulose. The magnitude of these peaks increased for 8 wt% of cellulose loading. The high intensity and narrow width of the peaks reflected the presence of crystalline regions in the polymer host, and amorphous regions developed when the intensity of the peaks became broader (Kaushik *et al*. 2010). Alternatively, amorphous regions were formed in the polymer host, and these regions grew after the addition of salt. According to a previous study, Su'ait *et al*. (2009a) stated that amorphous regions possess high ionic conductivity compared to the crystalline regions. Multiple diffraction peaks at around 2θ= 47°-50° correspond to (411) and (142) planes, respectively.

The width of the main peak at around 2θ~29° varied slightly in the presence of cellulose. A widening of the peaks indicated an increasing number of defects after the addition of salt (Azizi Samir *et al*. 2005). The peaks observed in the angular range of 30° to 50° became broader after the addition of Li salt. However, these peaks become narrow upon addition of cellulose. It is believed that the high crystallinity of cellulose fibers in

SPEs improved and enhanced the mechanical properties of SPE films. The crystallinity indices of MG49, SPEs without fibres, and SPEs with 4 wt% and 8 wt% were found to be 42.6%, 32.3%, 68.0%, and 78.3%, respectively. Based on data given in Table 1, a clear increase in the degree of crystallinity could be observed after the addition of cellulose.

Table 1. Crystallinity Index of SPEs

Sample / Peaks	Crystallinity Index (%)					
	22.5°	29.5°	39.4°	43.2°	47.5°	48.5°
MG49	-	42.6	41.4	41.4	51.0	33.6
0% cellulose	-	32.3	25.0	33.0	50.0	32.4
4% cellulose	16.2	68.0	22.4	29.2	50.5	46.3
8% cellulose	24.6	78.3	30.0	45.7	52.4	58.3

Ionic Conductivity

The ionic conductivity σ was conducted to analyze the effect of fibre loading in SPE and it was calculated according to the equation,

$$\sigma = \frac{l}{A \times R_b} \quad (2)$$

The bulk resistance R_b was obtained from the intercept on the real impedance axis (Z-axis), the film thickness l, and the contact area of the thin film [$A = \pi r^2 = \pi\ (0.80\ \text{cm})^2$] = 2.01 cm^2. Figure 7 shows a graph of conductivity for composite polymer electrolytes with a different percentage of fibre loading. All samples were analyzed at room temperature. The conductivity of polymer electrolytes was expected to increase with the addition of salt due to the increasing amount of the amorphous phase in the sample. The salt affected the overall conductivity through crystalline complex formation, intramolecular cross-linking of the polymer chains, and the degree of salt dissociation-number of charge carriers (Su'ait *et al*. 2009b). However, the conductivity of SPEs decreased after the addition of fibres (Table 2). This might have been due to the presence of OH groups in the cellulose bonding that disrupted the interaction between MG49 and the salt, thereby inhibiting the mobility of the salt ions (Azizi Samir *et al*. 2004a).

The introduction of cellulose had only a modest influence on the ionic conductivity of the composites (Table 2). The conductivity of the composites was reduced from 8.7×10^{-7} to 5.3×10^{-7} Scm^{-1} upon introduction of 2 wt% cellulose fibres. However, the values of the ionic conductivity remained higher than that of unfilled SPEs. The ionic conductivity decreased after cellulose loading due to ion accumulation, along with the aggregation of cellulose fibres in SPE and the effect of lithium salt crystallization.

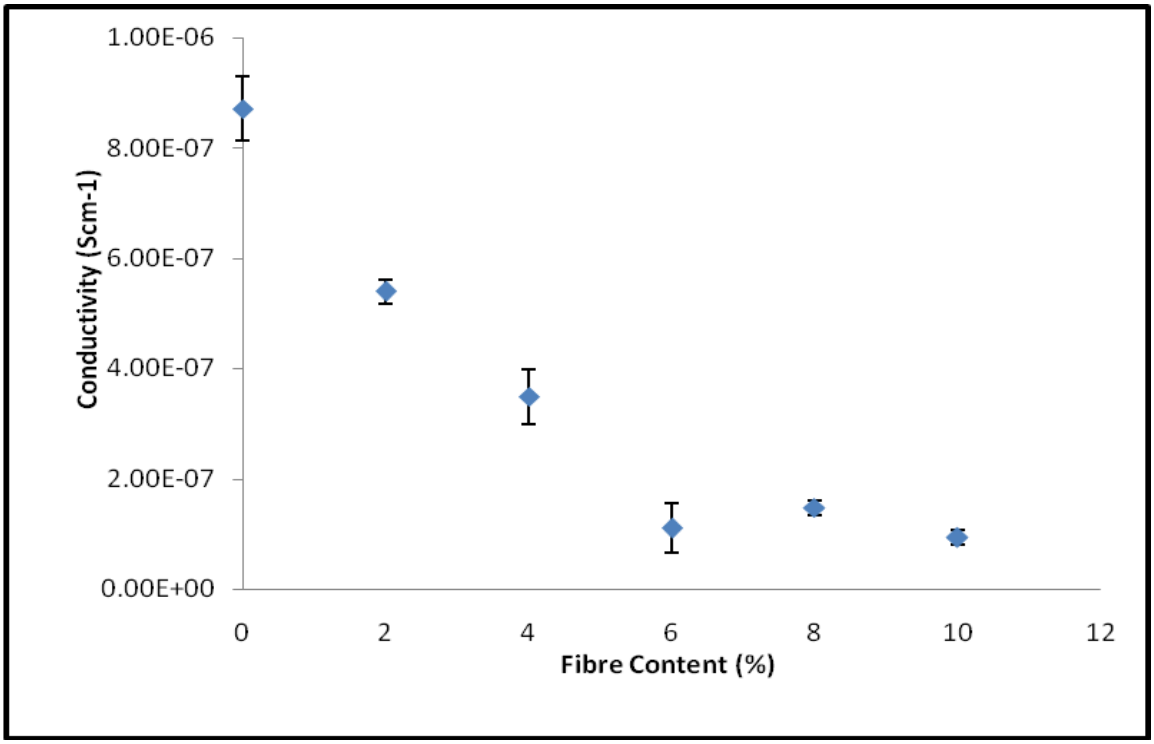

Fig. 7. Graph of Ionic conductivity of composite polymer electrolytes

Table 2. Ionic Conductivity of SPE MG49-$LiCF_3SO_3$-Cellulose

Cellulose Content, wt%	Conductivity, σ [Scm^{-1}]
0	8.7×10^{-7}
2	5.3×10^{-7}
4	3.5×10^{-7}
6	1.1×10^{-7}
8	1.5×10^{-7}
10	9.2×10^{-8}

Likewise, a decrease in the ionic conductivity upon addition of tunicin whiskers in poly(ethylene oxide) (PEO)-based electrolytes was also observed by Azizi Samir *et al*. (2004a, b), Alloin *et al*. (2010), and Schroers *et al*. (2004). According to Azizi Samir *et al.* (2005), the conductivity also tends to decrease due to i) the reduction of the relaxation time of polymer chains and ii) a decrease in the diffusion coefficient of both anions and cations. The difference in conductivity observed between filled and unfilled composites might be due to the existence of interactions between cellulose and MG49 or lithium salt (Alloin *et al*. 2010). Cellulose fibres contain hydroxyl groups, -OH, that interact with lithium cations, Li^+. Nevertheless, interactions between anions and the surface hydroxyl groups of cellulose fibres via hydrogen bonding decrease the mobility of the former (Azizi Samir *et al*. 2004a). Decreased mobility might also be due to the low dielectric constant of cellulose filler and favourable filler/matrix interactions. The highest conductivity for filled polymer electrolytes was obtained at a concentration of 2 wt% cellulose fibres, amounting to 5.3×10^{-7} $S \cdot cm^{-1}$. The conductivity gradually reduced with cellulose loading due to fibre agglomeration, which reduced the Li^+ ion mobility and thus the bulk conductivity. However, the reduction of the conductivity was insignificant compared to other SPEs without cellulose.

Morphological Investigation

The morphology of the polymer electrolytes was characterized using SEM. Figures 8a and 8b show the morphology of MG49 and the MG49/cellulose composite, respectively. Figures 8c, 8d, and 8e show SEM micrographs of MG49/Li without fibres, 4 wt% cellulose, and 8 wt% cellulose, respectively. Figure 8a shows an MG49 film with a rough morphology with some rumples. Differences in the phase structure can be observed due to the existence of dark and bright areas on the surface that represent the crystalline and the amorphous phase fraction, respectively. In Figure 8b, a homogeneous distribution of white dots was observed due to the good dispersion of cellulose in MG49. The white dots in Figure 8b can be interpreted as cellulose fibres in MG49 with no apparent aggregates (Alloin *et al.* 2010).

On blending with salt, the MG49 surface morphology became smoother compared to the original MG49 material. The smoother surface morphology was associated with a reduction in the degree of crystallinity of the polymer matrix after the addition of salt. This was due to the formation of coordinate bonds of lone pair electrons of oxygen atoms from MMA with Li^+ ions from the salt to form polymer complexes, as discussed in the ATR-FTIR characterization.

In Figure 8d and 8e, the surface became rough, which was associated with an increase in crystallinity as discussed in the XRD section. Some agglomeration occurred after more than 4 wt% of cellulose was added which contributed to the reduction in mechanical properties of SPEs (Fig. 8e).

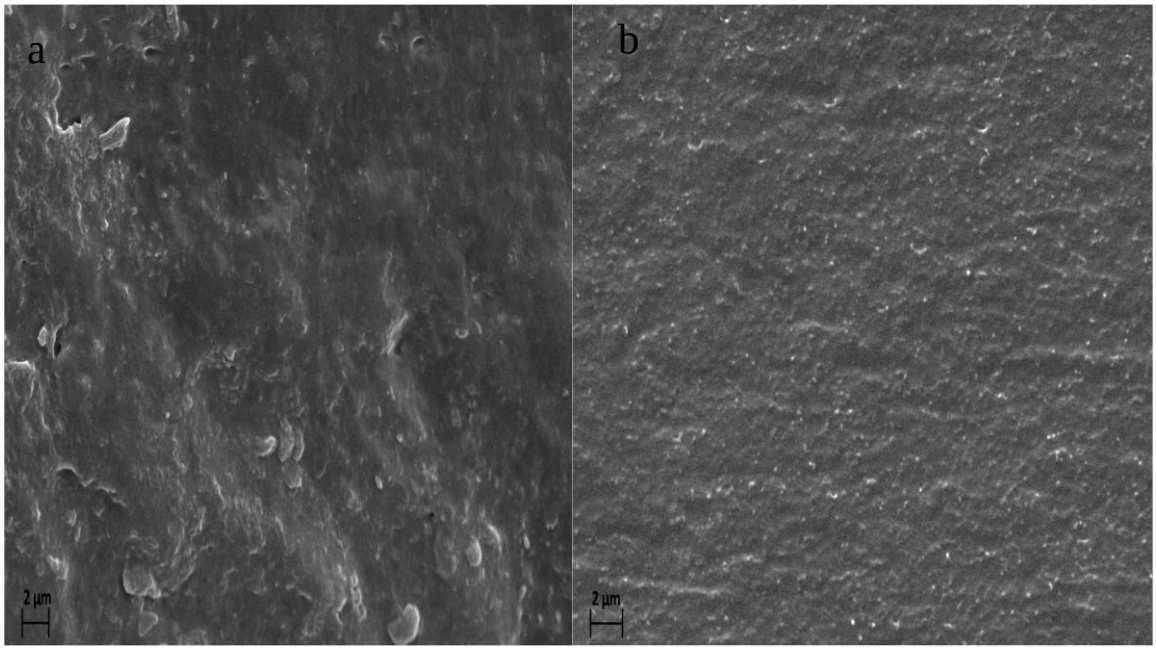

Fig. 8a & b. SEM micrographs of SPEs: a) MG49; b) MG49+fibre

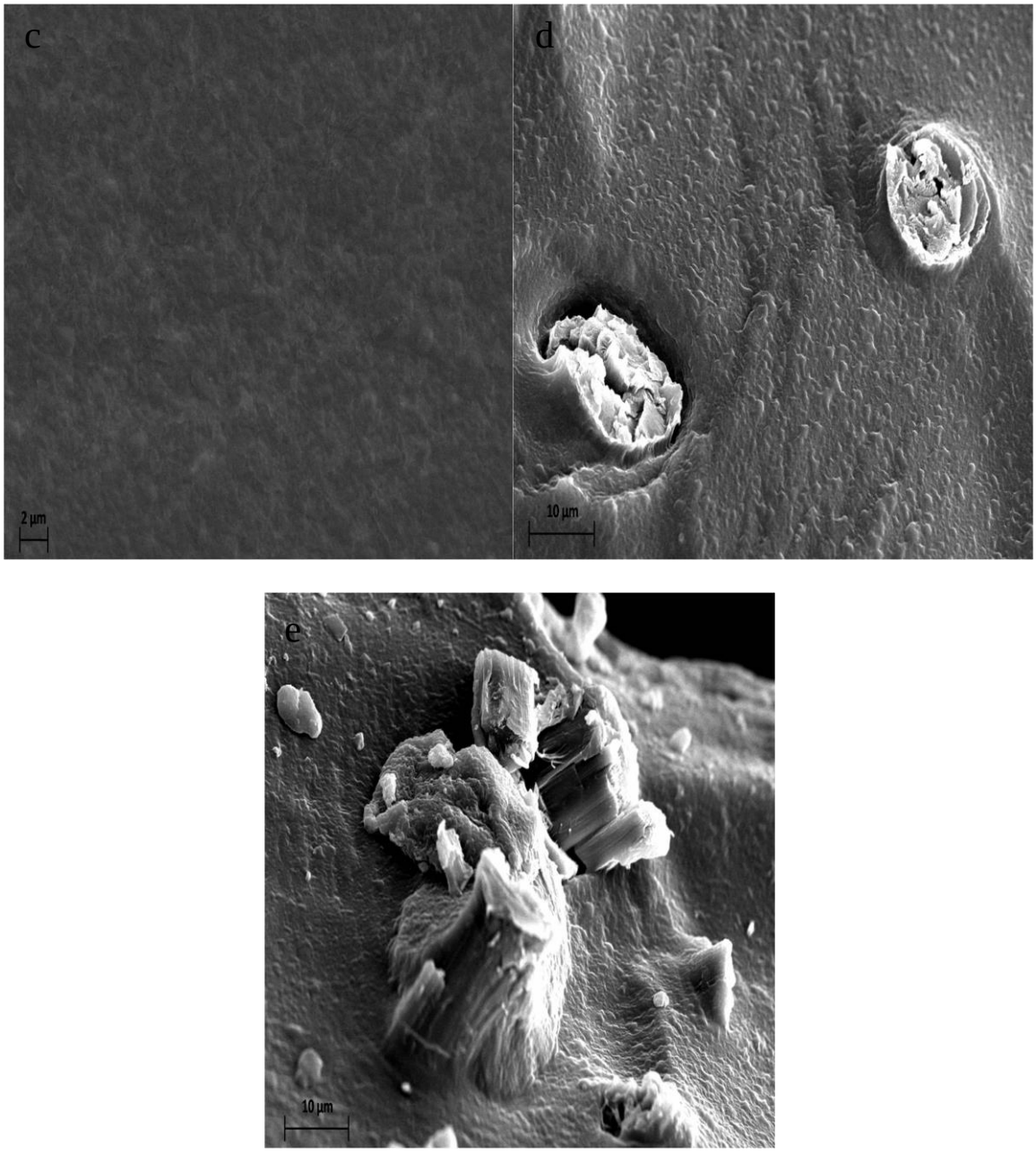

Fig. 8c, d, and e. SEM micrographs of SPEs: c) MG49+salt; d) MG49+salt+ 4 wt% fibre, and e) MG49+salt+ 8 wt% fibre

CONCLUSIONS

1. Cellulose fibres were successfully extracted from kenaf through a two-step chemical treatment: an alkali treatment and a bleaching process.
2. X-ray diffraction showed that the crystallinity of polymer complexes decreased after the addition of salt and increased upon addition of cellulose to SPEs.

3. The chemical treatment of kenaf fibres resulted in significant physical changes in the fibres. The diameter of the fibres was reduced from 125 µm to 6 µm after different stages of treatment.
4. Composite polymer electrolytes were prepared using MG49, $LiCF_3SO_3$, and cellulose fibres. The presence of cellulose fibres induced a weak decrease in the conductivity of SPEs that might be a result of interactions between cellulose and MG49 or salt. The highest value of ionic conductivity of SPE with cellulose was 5.3×10^{-7} Scm^{-1}. Cellulose can undergo some modification such as carboxymethyl cellulose to enhance its amorphous properties, hence increasing the conductivity.
5. The use of cellulose fibres as a reinforcing filler leads to high mechanical strength for SPEs, even at a small percentage of cellulose fibres. Values of 10.9 MPa and 995 MPa for tensile strength and Young's modulus, respectively, were achieved. The design of new polymer electrolytes, which combine both high ionic conductivity and good mechanical characteristics, is feasible using this approach.

ACKNOWLEDGMENTS

The authors would like to express their gratitude towards Universiti Kebangsaan Malaysia for the permission for this research to be carried out within the university premises. Financial support was received from the Ministry of Higher Education under research grant numbers ERGS/1/2012/STG01/UKM/02/4 and UKM-DLP-2012-021 and in the form of Zamalah Universiti Penyelidikan from Universiti Kebangsaan Malaysia.

REFERENCES CITED

Ahmad, A., Rahman, M. Y. A., Su'ait, M. S., and Hamzah, H. (2011). "Study of MG49-PMMA based solid polymer electrolyte," *The Open Materials Science Journal* (5), 170-177.

Alemdar, A., and Sain, M. (2008)."Biocomposites from wheat straw nanofibres: Morphology, thermal and mechanical properties," *Composites Science and Technology* 68(2), 557-565.

Alloin, F., D'Aprea, A., Kissi, N. E., Dufresne, A., and Bossard, F. (2010). "Nanocomposite polymer electrolytes based on whisker or microfibrils polyoxyethylene nanocomposites," *Electrochimica Acta* 55(18), 5185-5194.

Azizi Samir, M. A. S., Alloin, F., Gorecki, W., Sanchez, J. Y., and Dufresne, A. (2004a). "Nanocomposite polymer electrolytes based on poly(oxyethylene) and cellulose nanocrystal," *Journal of Physical Chemistry* 108(30), 10845-10852.

Azizi Samir, M. A. S., Mateos, A. M., Alloin, F., Sanchez, J. Y., and Dufresne, A. (2004b). "Plasticized nanocomposite polymer electrolytes based on poly(oxyethylene) and cellulose whiskers," *Electrochimica Acta* 49(26), 4667-4677.

Azizi Samir, Chazeau, L., Alloin, F., Cavaille, J.-Y., Dufresne, A., and Sanchez, J.-Y. (2005). "POE-based nanocomposite polymer electrolytes reinforced with cellulose whiskers," *Electrochimica Acta* 50(19), 3897-3903.

Bismark, Mishra, S., and Lampke, T. (2005). "Plant fibres as reinforcement for green composites," in *Natural Fibres Biopolymers and Biocomposites*, Vol. 2, A. K. Mohanty, M. Misra, and L. T. Drzal (eds.), CRC Press, Boca Raton.

Chiappone, A., Nair, J. R., Gerbaldi, C., Jabbour, L., Bongiovanni, R., and Zeno, E. (2011). "Microfibrillated cellulose as reinforcement for Li-ion battery polymer electrolytes with excellent mechanical stability," *Journal of Power Sources* (196), 104-111.

Kamisan, A. K., Kudin, T. I. T., Ali, A. M. M. and Yahya, M. Z. A. (2011). "Electrical and physical studies on 49% methyl grafted natural rubber-based composite polymer gel electrolytes," *Electrochimica Acta* (57), 207-211.

Kargarzadeh, H., Ahmad, I., Abdullah, I., Dufresne, A., Yasmine, Z. S., and Rasha, M. S. (2012). "Effects of hydrolysis conditions on the morphology, crystallinity, and thermal stability of cellulose nanocrystals extracted from kenaf bast fibres," *Cellulose* 19(3), 855-866.

Kaushik, A., Singh, M., and Verma, G. (2010). "Green nanocomposite based on thermoplastic starch and steam exploded cellulose nanofibrils from wheat straw," *Carbohydrate Polymer* 82(2), 337-345.

Labuschagne, P. W., Germishuizen, W. A., Verryn, S. M. C., and Molman, F. S. (2008). "Improved oxygen barrier performance of poly(vinyl alcohol) films through hydrogen bond complex with poly(methyl vinyl ether-co-maleic acid," *European Polymer Journal* (44), 2146-2152.

Latif, F., Aziz, M., Katun, N., Ali, A. M. M., and Yahya, M. Z. (2006). "The role and impact of rubber in poly(methyl methacrylates)/lithium triflate electrolytes," *Journal of Power Sources* (159), 1401-1404.

Li, R., Fei, J., Cai, Y., Li, Y., Feng, J., and Yao, J. (2009). "Cellulose whiskers extracted from mulberry: A novel biomass production," *Carbohydrate Polymers* 76(1), 94-99.

Low, S.P., Ahmad, A. and Rahman, M. Y. A. (2010). "Effect of ethylene carbonate plasticizer and TiO_2 nanoparticles on 49% poly(methyl methacrylate)-grafted natural rubber-based polymer electrolytes," *Ionic* (16), 821-826.

Mobarak, N. N., Ahmad, A., Abdullah, M. P., Ramli, N., and Rahman, M. Y. A. (2013). "Conductivity enhancement via chemical modification of chitosan based green polymer electrolyte," *Electrochimica Acta* 92, 161-167.

Nair, J. R., Gerbaldi, C., Chiappone, A., Zeno, E., Bongiovanni, R., Bodoardo, S., and Penazzi, N. (2009). "UV-cured polymer electrolytes membranes for Li-cells: Improved mechanical properties by a novel cellulose reinforcement," *Electrochemistry Communication* (11), 1796-1798.

Nik Aziz, N. A., Idris, N.K., and M. I. N. Isa. (2010). "Proton conducting polymer electrolytes of methylcellulose doped ammonium fluoride: Conductivity and ionic transport studies," *International Journal of the Physical Sciences* 5(6), 748-752.

Pandey, J. K., Kim, C. S., Chu, W. S., Caroline S. L., Jang, D. Y. and Ahn, S. Y. (2009). "Evaluation of morphological architecture of cellulose chains in grass during conversion from macro to nano dimensions," *e-Polymers*, no. 102.

Pawlicka, A., Danczuk, M., Wieczorek, W., and Zygadlo- Monikowska, E. (2008). "Influence of plasticizer type on the properties of polymer electrolytes based on chitosan," *Journal of Physical Chemistry A* 112(38), 8888-8895.

Regiani, A. M., Machado, G. O., LeNest, J. F., Gandini, A., and Pawlicka, A. (2001)."Cellulose derivatives as solid electrolyte matrixes," *Macromolecular Symposia* 175, (1), 45-54.

Rout, J., Tripathy, S. S., Nayak, S. K., Misra, M., and Mohanty, A. K. (2001). "Scanning electron microscopy study of chemically modified coir fibres," *Journal of Applied Polymer Science* 79(7), 1169-1177.

Rowell, R. M., and Stout, H. P. (1998). *Handbook of Fibres Chemistry*, 2nd Ed., Marcel Dekker, New York.

Rozali, M. L. H, Samsudin, A. S., and Isa, M. I. N. (2012). "Ion conducting mechanism of carboxy methylcellulose doped with ionic opant salicylic acid based solid polymer electrolytes," *International Journal of Applied Science and Technology* 2(4), 113-121.

Samsudin, A. S., and Isa, M. I. N. (2012). "Structural and ionic transport study on CMC doped NH_4Br: A new type of biopolymer electrolytes," *Journal of Applied Sciences* 12(2), 174-179.

Schroers, M., Kokil, A., and Weder, C. (2004). "Solid polymer electrolytes based on nanocomposites of ethylene oxide-epichlorohydrin copolymers and cellulose whiskers," *Journal of Applied Polymer Science* 93(6), 2883-2888.

Siqueira, G., Abdillahi, H., Bras, J., and A. Dufresne. (2010). "High reinforcing capability cellulose nanocrystals extracted from *Syngonanthus nitens* (Capim Dourado)," *Cellulose* 17(2), 289-298.

Su'ait, M. S., Ahmad, A., and Rahman, M. Y. A. (2009a). "Ionic conductivity studies of 49% poly(methyl methacrylate)-grafted natural rubber-based solid polymer electrolytes," *Ionics* 15(4), 497-500.

Su'ait, M. S., Ahmad, A., Hamzah, H., and Rahman, M. Y. A. (2009b). "Preparation and characterization of PMMA–MG49–$LiClO_4$ solid polymeric electrolyte," *Journal Physics D: Applied Physics* 42(5), 1-5.

Swingle, R. S., Urias, A. R., Doyle, J. C., and Voight, R. L. (1978). "Chemical composition of kenaf forage and its digestibility by lambs and in vitro," *Journal Animal Sciences* 46(5), 1346-1350.

Article submitted: April 17, 2013; Peer review completed: June 19, 2013; Revised version received and accepted: September 16, 2013; Published: October 1, 2013.